Springer

KSME

Journal of Mechanical Science and Technology 32 (8) (2018) 3515~3521
www.springerlink.com/content/1738-494x(Print)/1976-3824(Online)
DOI 10.1007/s12206-018-0702-y

Active vibration control based on modal controller considering structure-actuator interaction †

Jinjun Jiang[1], Weijin Gao[1,*], Liang Wang[2], Zhaohua Teng[1] and Yongguang Liu[2]

[1]*Institute of Wind Tunnel Engineering Technology, China Academy of Aerospace Aerodynamics, Beijing, 100074, China*
[2]*School of Automation Science and Electrical Engineering, Beihang University, Beijing, China*

(Manuscript Received October 15, 2017; Revised February 9, 2018; Accepted May 6, 2018)

Abstract

Active vibration control to suppress structural vibration of the flexible structure is investigated based on a new control strategy considering structure-actuator interaction. The experimental system consists of a clamped-free rectangular plate, a controller based on modal control switching, and a magnetostrictive actuator utilized for suppressing the vibrations induced by external excitation. For the flexible structure, its deformation caused by the external actuator will affect the active control effect. Thus interaction between structure and actuator is considered, and the interaction model based on magnetomechanical coupling is incorporated into the control system. Vibration reduction strategy has been performed resorting to the actuator in optimal position to suppress the specified modes using LQR (linear quadratic regulator) based on modal control switching. The experimental results demonstrate the effectiveness of the proposed methodology. Considering structure-actuator interaction (SAI) is a key procedure in controller design especially for flexible structures.

Keywords: Flexible structures; Vibration suppressing; Structure-actuator interaction; Modal control switching

1. Introduction

As is well known, an effective approach in making some structures more efficient is to reduce their weight especially in the area of aerospace. As a result, these structures are typically made thin. However, some components of these structures are prone to experiencing excessive vibrations such as flutter and fatigue failure. In order to solve these vibration problems, both passive and active vibration control approaches have been developed and implemented. For instance, the inertial actuator as a usual vibration control method [1, 2], is a mass supported on a spring and damper. Due to its structural features, it sometimes is not as lightweight as is required. Subsequently, active actuators made of smart material are applied onto the flexible structures. Many investigators have implemented experimental research for active vibration control employing smart material actuators [3-8].

Compared to piezoelectric ceramic material (PZT) and shape memory alloy (SMA), giant magnetostrictive material (GMM) has some advantages such as generation of large forces, high load bearing capability, high magnetomechanical coupling, and rapid reaction. In view of the advantages of GMM, giant magnetostrictive actuators are a promising technology in active vibration control [9, 10]. Moon and Lim have designed a linear magnetostrictive actuator (MSA) using Terfenol-D, and analyzed the characteristics of the actuator by implementing a series of experimental and numerical tests which confirmed that the linear MSA had a good control performance [5]. Braghin and Cinquemani introduced a linear model of magnetostrictive actuators that was valid in a range of frequencies below 2 kHz, and the model was verified through experiments [9]. Zhou and Zheng presented a nonlinear constitutive model-based vibration control system for giant magnetostrictive actuators, and the effectiveness of a real control system for suppressing a vibration was demonstrated by a case study with negative velocity feedback [11]. However, a more widespread application for giant material actuators (GMA) is restrained by an inherent property of GMM. Therefore, researchers have started to focus on the characteristics of GMA, such as nonlinear hysteresis phenomena [12-15] which can cause the instability of the system. The nonlinear behaviors can be modeled by a range of approaches [16-20]. Liu and Zhang constructed a dynamic model in a given rate range for a rate-dependent hysteresis system, and a PID control combined with feedforward compensation was employed on a giant magnetostrictive actuator. The results gotten by simulations and experiments indicated the effectiveness of the proposed methods [21]. Aljanaideh and Rakheja proposed a phenomenological hysteresis model for the hysteresis nonlinearities of

*Corresponding author. Tel.: +86 18810524844, Fax.: +86 1068741330
E-mail address: gwj_008@126.com
† Recommended by Associate Editor Gyuhae Park

Table 1. Parameters of GMM.

Parameter	Value
Young's modulus (N/m^2)	(2.5~10)×10^{10}
Tensile strength (MPa)	28
Compression strength (MPa)	700
Magnetoelastic coupling factor	0.75
Relative magnetic conductivity	3~15
Resistivity (Ω·m)	60×10^{-8}

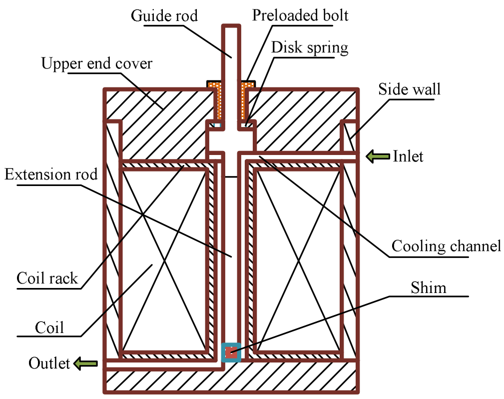

Fig. 1. GMA model.

a magnetostrictive actuator, and the model effectively describe the nonlinear hysteresis properties of the actuator [22]. From previous investigations of vibration control systems, mostly the nonlinear behaviors of actuators are considered by using compensation algorithms, with little consideration of the relationship between actuator and structure that is also important for the whole system. In Ref. [23], computational models considering the interaction between the GMA and structure were developed, and the results demonstrated that consideration of the CSI and the dynamics of the GMA can improve the performance of a controller significantly. In this paper, the main purpose is to demonstrate the control strategy with considering the interaction between the actuator and the structure for a flexible structure, thus the nonlinear behavior for GMA like rate-dependency hysteresis will not be described.

For flexible structures, application of an external force will generate a reactive force to the object producing the external force. For smart material such as piezoelectric/piezomagnetic actuators, this interaction may affect the performance of these actuators. In this work, in order to validate the proposed method, an interaction model between structure and actuator is derived and constructed. Based on the model, the experiment is implemented utilizing the proposed control strategy. The experiment results demonstrate the effectiveness of the control model.

2. Model establishment of giant magnetostrictive actuator

In order to improve the control efficiency, the actuating

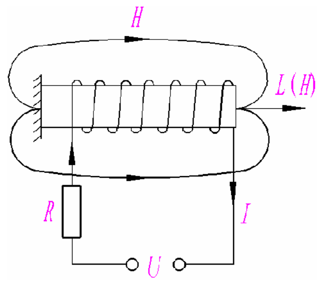

Fig. 2. Equivalent circuit of GMA.

principle of the actuator should be studied. A giant magnetostrictive actuator (GMA) is used in this paper as shown in Fig. 1 and the parameters of GMM (giant magnetostrictive material) are shown in Table 1.

2.1 Positive effect of GMA

When the voltage is applied to the ends of a coil, GMM will produce a deformation along the axial direction due to the Joule effect. This process is also named the "positive effect" and is shown in Fig. 2.

As is well known, magnetomotive forces (briefly named MMF) can be defined by their forms, and the two of them are given as follows

$$\begin{cases} MMF = NI \\ MMF = R_m \Phi \end{cases} \tag{1}$$

where N is the number of coil turns; I is the coil current; R_m is magnetic reluctance; and Φ is the magnetic flux. Here eddy current effect is neglected. According to Eq. (1), we can get that

$$\Phi = \frac{NI}{R_m}. \tag{2}$$

Furthermore, the output force of GMM can be expressed by

$$F = \Phi K_F = \Phi \frac{1}{d_{33}} \tag{3}$$

where K_F is the interaction coefficient between force and flux and d_{33} is piezomagnetic strain constant. Substituting Eq. (2) into Eq. (3), a new form with respect to the current is written as

$$F = \frac{NIK_F}{R_m} = \frac{NI}{R_m d_{33}} = \frac{NU}{RR_m d_{33}}. \tag{4}$$

2.2 Inverse effect of GMA

Aside from the positive effect of GMM, there also exists an inverse effect named the "Villari effect" shown in Fig. 3. When a force acts on the end of GMM, the voltage of the coil

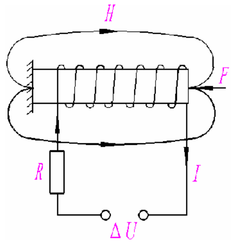

Fig. 3. Equivalent circuit of inverse effect.

will be changed.

For GMM, constitutive equation is given by

$$\begin{cases} \varepsilon = \dfrac{\sigma}{E} + d_{33}H \\ B = d_{33}\sigma + \mu^{\sigma} H \end{cases} \tag{5}$$

where ε, σ and E are strain, stress and elastic modulus, respectively. B, H and μ^{σ} are magnetic induction, magnetic field strength and magnetic conductivity, respectively. Moreover, according to the Faraday theorem, the induction voltage can be described in the following form

$$\Delta U = N d_{33} S E \frac{d\varepsilon}{dt} + L\frac{dI}{dt} \tag{6}$$

where S is the cross-sectional area of the GMM rod, and L is the induction coefficient. From Eq. (6), it can be seen that the induction voltage has a relation with the strain change ratio and the current change ratio.

3. Structure-actuator interaction model

For an active control system with an intelligent material actuator, theoretically only the actuator has a control effect on the structure, and the structure (i.e. the controlled object) has no influence on the actuator. However, especially for intelligent material, the structure will produce an opposing force to the actuator. The control stability is then destroyed due to the inverse effect. It is important that structure-actuator interaction (SAI) should be considered when a control system is designed including intelligent materials such as piezoelectricity and piezomagnetism. SAI will be described as follows.

When GMM is driven by voltage, it will generate axial displacement which satisfies the material mechanics theory

$$x = \varepsilon l_m \tag{7}$$

where x is axial displacement; l_m is the length of the GMM rod. According to Eq. (7), the change rate of axial displacement can then be expressed by

$$\frac{dx}{dt} = l_m \frac{d\varepsilon}{dt}. \tag{8}$$

In addition, Eq. (4) can be shown in the form of current

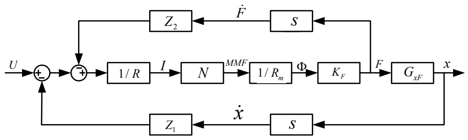

Fig. 4. System model considering SAI.

changing with respect to time, thus Eq. (6) also can be written as

$$\Delta U = \left(\frac{N d_{33} S E}{l_m}\right)\frac{dx}{dt} + \left(L\frac{R_m}{NK_F}\right)\frac{dF}{dt}. \tag{9}$$

Due to the significant changes for some parameters such as E, d_{33} and μ^{σ} under the action of pressure and temperature, correction coefficients will be introduced into Eq. (9), thus changing it to

$$\Delta U = \gamma_1\left(\frac{N d_{33} S E}{l_m}\right)\frac{dx}{dt} + \gamma_2\left(L\frac{R_m}{NK_F}\right)\frac{dF}{dt} \tag{10}$$

where γ_1 and γ_2 are correction factors. From Eq. (10), it can be seen that $\gamma_1\left(\frac{N d_{33} S E}{l_m}\right)$ and $\gamma_2\left(L\frac{R_m}{NK_F}\right)$ only have relations with the characteristic parameters of GMM, so Eq. (10) is simplified as

$$\Delta U = Z_1\frac{dx}{dt} + Z_2\frac{dF}{dt} \tag{11}$$

where $Z_1 = \gamma_1\left(\frac{N d_{33} S E}{l_m}\right)$ and $Z_2 = \gamma_2\left(L\frac{R_m}{NK_F}\right)$. Note Z_1 that Z_2 and are not constants due to the correction factors, and the two values are only applied to the current case and gotten by identifying trial results.

In order to indicate that some parameters of GMM influence the parameter K_F, another correction coefficient is introduced. Substituting Eq. (11) into Eq. (4), the output force is given by considering structure-actuator interaction

$$F = \gamma_3\frac{NIK_F}{R_m} = \frac{\gamma_3\left(U - Z_1\frac{dx}{dt} - Z_2\frac{dF}{dt}\right)NK_F}{RR_m}. \tag{12}$$

From Eq. (12), we can see that the coefficient $\frac{\gamma_3 NK_F}{RR_m}$ only has relation with the material characteristic parameters of GMA. Therefore the coefficient is replaced here by Z_3, and Eq. (12) also can be written as

$$F = Z_3 U - Z_1 Z_3 \dot{x} - Z_2 Z_3 \dot{F}. \tag{13}$$

According to the equations shown above, the system model is shown in Fig. 4.

4. Control algorithm

In this paper, a hybrid modal space control method is proposed, and the process of this method is derived by following equations. Here, the governing equation of motion for a structure with piezoelectric actuators is written as

$$M\ddot{x} + Kx = u \tag{14}$$

where u represents the load due to actuation, M is the mass matrix, K is the stiffness matrix, and x contains node displacements. In order to realize decoupling, the displacement of nodes in physical space will be transformed to modal space according to expansion theorem

$$x = \phi q \tag{15}$$

where ϕ is the vector of mode shape, and q is the corresponding modal coordinate. Substituting Eq. (15) into Eq. (14), it can be gotten by

$$M\phi\ddot{q} + k\phi q = u. \tag{16}$$

In this paper, normalization of mass is employed and Eq. (16) can be written in the following form as

$$\ddot{q} + \Omega q = \phi^T u. \tag{17}$$

Then, for any order natural frequency, the governing equation is given as follows

$$\ddot{q}_i + \omega_i^2 q_i = \phi_i^T u = F_i \tag{18}$$

where ω_i is the natural frequency and F_i is the actuating force.

4.1 Independent modal space control

According to the active control principle, the control force can be written as

$$F_i = -g_i q_i - h_i \dot{q}_i \qquad i = 1, 2, \cdots, N \tag{19}$$

where g_i is displacement gain and h_i is speed gain. Then the closed loop formed in modal space is expressed by

$$\ddot{q}_i + h_i \dot{q}_i + \left(g_i + \omega_i^2\right) q_i = 0. \tag{20}$$

From Eq. (20), it can be seen that the governing equation of each order is in a separate state. It is easy to design the control law, and the real control signal can be written as

$$u = -\sum_{i=1}^{N} M\phi_i \left(g_i q_i + h_i \dot{q}_i\right) \tag{21}$$

4.2 Dependent modal space control

For dependent modal space control, let F_i be

$$F_i = -\sum_{s=1}^{N} \left(g_{is} q_s + h_{is} \dot{q}_s\right) \qquad i = 1, 2, \cdots, N \tag{22}$$

and the closed loop form considering the external control is given by

$$\ddot{q}_i + \sum_{s=1}^{N} h_{is} \dot{q}_s + \sum_{s=1}^{N} \left(g_{is} + \omega_i^2 \delta_{is}\right) q_s = 0 \tag{23}$$

where h_{is} and g_{is} are the speed gain and the displacement gain in modal space, respectively. In addition, here δ_{is} can be given by $\delta_{is} = \begin{cases} 0, & i \neq s \\ 1, & i = s \end{cases}$. The real control signal is shown in the form as

$$u = M\phi F = \sum_{i=1}^{N} M\phi_i F_i = -\sum_{i=1}^{N} \sum_{s=1}^{N} M\phi_i F_i \left(g_{is} q_s + h_{is} \dot{q}_s\right). \tag{24}$$

4.3 Hybrid modal space control

In order to describe hybrid modal space control, let $h = \begin{bmatrix} q & \dot{q} \end{bmatrix}^T$, Eq. (17) can be written in the form of the state space

$$\dot{h} = Ah + Bu \tag{25}$$

where $A = \begin{bmatrix} 0 & I \\ -\Omega & 0 \end{bmatrix}, B = \begin{bmatrix} 0 \\ \phi^T \end{bmatrix}$.

In modal space, according to Eq. (25), we can get that

$$\dot{h}_i = A_i h_i + B_i u_i \qquad \left(i = 1, 2, \cdots, n\right) \tag{26}$$

where $A_i = \begin{bmatrix} 0 & I \\ -\omega_i^2 & 0 \end{bmatrix}, B_i = \begin{bmatrix} 0 \\ \phi_i^T \end{bmatrix}$.

For dependent modal space control, the linear quadratic index can be written as

$$J = \frac{1}{2} \int_0^\infty \left(h^T Q h + u^T R u\right) dt \tag{27}$$

where Q is a diagonal matrix and R is a symmetric positive definite matrix.

Similarly to independent modal space control, the linear quadratic index can be written as

$$J_i = \frac{1}{2} \int_0^\infty \left(h_i^T Q_i h_i + u_i^T r_i u_i\right) dt \qquad \left(i = 1, 2, \cdots, n\right) \tag{28}$$

where Q_i is the second order diagonal matrix and r_i is a constant.

In accordance with optimal control theory, the optimal control force is expressed as

$$\begin{cases} F_c = -R^{-1}B^T G(t)h \\ F_{ci} = -r_i^{-1}B_i^T G_i(t)h_i \end{cases} \tag{29}$$

where $G(t)$ and $G_i(t)$ are obtained from Riccati equations as shown in Eq. (30).

$$\begin{cases} -A^T G(t) - G(t)A + G(t)BR^{-1}B^T G(t) - Q = 0 \\ -A_i^T G_i(t) - G_i(t)A + G_i(t)B_i r_i^{-1}B_i^T G_i(t) - Q_i = 0 \end{cases} \tag{30}$$

in addition, Eq. (30) is easy to be solved by MatLab.

In the process of the closed loop control, a modal tracking strategy is taken to determine control-switching, which is described as follows. According to the principle of mode superposition, a definition with respect to modal coordinate is given by

$$W_h = \sum_{i=1}^{n} \|h_i\| \tag{31}$$

where W_h represents the aggregate weighting of the controlled modes. Moreover, one may define

$$\Gamma_i = \frac{\|h_i\|}{W_h} \tag{32}$$

where Γ_i denotes the contribution of i-th mode to the aggregate weighting. Obviously, if the controlled mode needs to be determined, one condition should be satisfied by

$$\Gamma_j = \max(\Gamma_1, \Gamma_2, \cdots, \Gamma_n) \tag{33}$$

where Γ_j indicates the chosen mode that is used to determine feedback gain. Fig. 5 shows the program flow chart of hybrid modal space control.

Here, the control program shown in Fig. 5 is called modal control switching. In control process, the actuator output will produce a appropriate signal according to the modal tracking strategy.

5. Experiments and results

With the actuator model completed and control algorithm considering SAI designed, it is of importance to experimentally evaluate the proposed method for active vibration control. In this section, an experimental setup is described, and experimental results are presented and discussed.

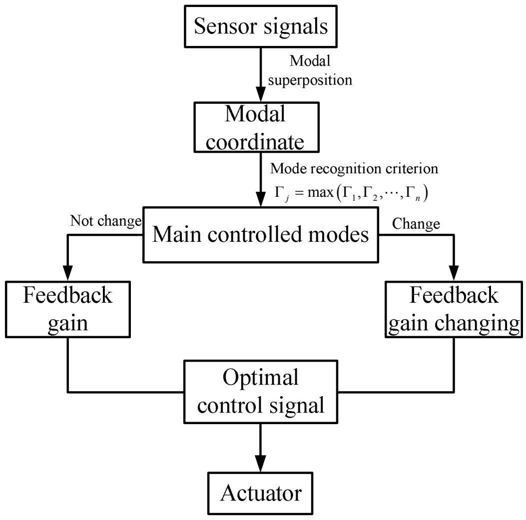

Fig. 5. The program flow chart of hybrid modal space control.

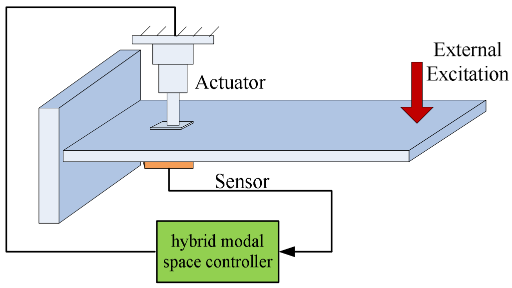

Fig. 6. Diagrammatic sketch of the experimental system.

5.1 Experimental setup

In this experiment, the actuator is positioned near the end of the rectangular plate and is mounted on a support. The sensor is placed on the opposite side of the actuator. Fig. 6 shows a diagrammatic sketch of the experimental system.

The system shown in Fig. 6 is realized by adopting three means. Firstly, the relative parameters of actuator are acquired by some trials, the real actuator is seen in Fig. 7. Secondly, the rectangular plate with one side clamped is constructed by using virtual prototyping technology (VPT). Thirdly, the hybrid modal space control algorithm is implemented using Matlab/Simulink.

From Eq. (13), note that SAI needs three parameters Z_1, Z_2 and Z_3. Through addressing the trial results, these are given by $Z_1 = 1200, Z_2 = 0.045, Z_3 = 0.204$. Besides, it is also noted that Eq. (13) can be divided into two models according to the computation requirements for a control system. The first model is the full expression of SAI given in Eq. (13). The second model is an ideal linear actuator, which neglects SAI. This model, $F = Z_3 U$, is usually used. In subsequent simulations, the vibration suppression results will be given considering these two models respectively.

In addition, some relative parameters of the plate structure are listed in Table 2.

Table 2. Parameters of the plate structure.

Parameter	Value
Length (mm)	100
Width (mm)	50
Thickness (mm)	2
Density (kg/m^3)	2800
Young's ratio (GPa)	70
Damping ratio	0.0002

Table 3. Natural frequencies of the plate structure.

Number of order	1	2	3	4	5
Natural frequency (Hz)	24.2	38.2	61.8	81.3	96.1

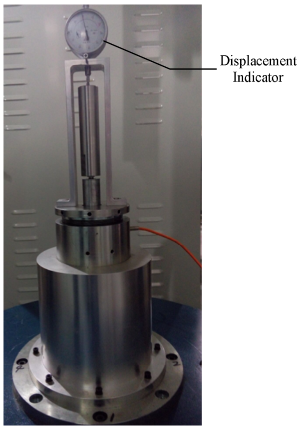

Fig. 7. Giant material actuator.

5.2 Experimental results and discussion

For the aim of active vibration control, only the first five modes are considered, and their natural frequencies are given in Table 3.

In this section, several experimental results are presented for illustrating the influence of interaction models on the control system. For exciting the mode shapes of the plate structure, a concentrated load is applied at a central location on the free end of the plate, which is a sine sweep excitation signal with an amplitude of 100 N and a frequency of 0~200 Hz. In the first experimental results, the first two modes are controlled and the remaining three modes are regarded as residual modes, as shown in Fig. 8.

In the second set of experimental results, the first three modes are controlled and the remaining two modes are considered as residual modes, which is shown in Fig. 9.

As can be seen in these two figures, the vibrations are suppressed by using an additional actuator. In Figs. 8 and 9, it can be seen that the plate with SAI considered has more "stiffer" than the one without SAI considered. When the first two modes are controlled, the vibrations are suppressed by using the control method without SAI. But when the first three modes are controlled, for the response of the third order frequency, the control method without SAI does not act. The

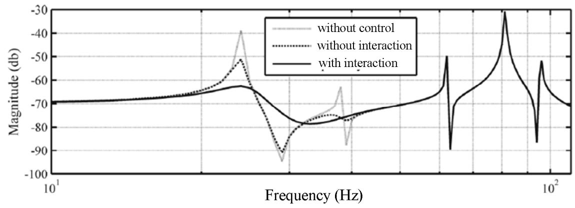

Fig. 8. Frequency response of the plate.

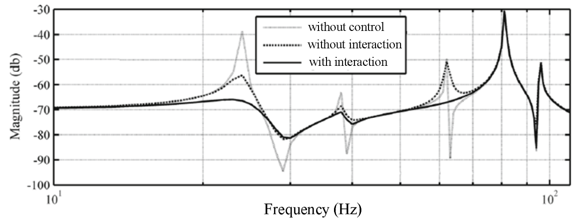

Fig. 9. Frequency response of the plate.

proposed approach, meanwhile, effectively suppresses vibration suppressing effectiveness whether in either the first experimental results or in the second experimental results.

6. Conclusions

This work presented in this paper indicates that the proposed active vibration control with SAI (structure-actuator interaction) considered can be utilized successfully to suppress vibrations of a flexible plate structure. In this investigation, the SAI model is constructed according to magnetomechanical coupling, based on which the controller is designed. In order to improve the control effect, a modal control switching strategy is employed. According to the proposed methodology, an experimental setup is established to verify the feasibility of the method. The experimental results show that the stiffness effect of the plate structure could be increased and the amplitudes of the plate vibration are reduced more effectively. Furthermore, the present methodology can be extended to other flexible structures.

Acknowledgments

This work is supported by National Natural Science Fund (No. 11272026).

References

[1] L. Benassi, S. J. Elliott and P. Gardonio, Active vibration isolation using an inertial actuator with local force feedback control, *Journal of Sound and Vibration*, 276 (2004) 157-179.

[2] I. Maciejewski and T. Krzyzynski, Method of selecting vibro-isolation properties of vibration reduction systems, *Journal of Mechanical Science and Technology*, 30 (4) (2016) 1497-1505.

[3] S. B. Choi, Alleviation of chattering in flexible beam control

via piezofilm actuator and sensor, *AIAA J.*, 33 (1995) 564-567.

[4] S. C. Mou, Structure design and stepping characteristics analysis of the biaxial piezoelectric actuator stage using a thin-disc piezoelectric actuator, *Advances in Mechanical Engineering* (2014) 1-16.

[5] S. J. Moon et al., Structural vibration control using linear magnetostrictive actuators, *Journal of Sound and Vibration*, 302 (2007) 875-891.

[6] Z. Butt et al., Generation of electrical energy using lead zirconate titanate (PZT-5A) piezoelectric material: Analytical, numerical and experimental verification, *Journal of Mechanical Science and Technology*, 30 (8) (2016) 3553-3558.

[7] A. G. Olabi and A. Grunwald, Design and application of magnetostrictive materials, *Materials and Design*, 22 (2008) 469-483.

[8] T. Zhang et al., Giant magnetostrictive actuators for active vibration control, *Smart Material and Structures*, 13 (2004) 473-477.

[9] F. Braghin, S. Cinquemani and F. Resta, A model of magnetostrictive actuators for active vibration control, *Sensors and Actuators A: Physical*, 165 (2011) 342-350.

[10] F. Braghin, S. Cinquemani and F. Resta, A low frequency magnetostrictive inertial actuator for vibration control, *Sensors and Actuators A: Physical*, 180 (2012) 67-74.

[11] H. M. Zhou, X. J. Zheng and Y. H. Zhou, Active vibration control of nonlinear giant magnetostrictive actuators, *Smart Materials and Structures*, 15 (2006) 792-798.

[12] M. J. Dapino et al., A coupled magnetomechanical model for magnetostrictive transducers and its application to Villari-effect sensors, *Journal of Intelligent Material Systems and Structures*, 13 (11) (2002) 737-747.

[13] S. Valadkhan, K. Morris and A. Khajepour, Review and comparison of hysteresis models for magnetostrictive materials, *Journal of Intelligent Material Systems and Structures*, 20 (2) (2009) 131-142.

[14] M. J. Dapino et al., A coupled structural-magnetic strain and stress model for magnetostrictive transducers, *Journal of Intelligent Material Systems and Structures*, 11 (2000) 135-151.

[15] M. J. Dapino, R. C. Smith and A. B. Flatau, Structural-magnetic strain model for magnetostrictive transducers, *IEEE Transactions on Magnetics*, 36 (3) (2000) 545-556.

[16] J. P. Lien et al., Modeling piezoelectric actuators with hysteretic recurrent neural networks, *Sensors and Actuators A*, 163 (2) (2010) 516-525.

[17] W. S. Oates and R. C. Smith, Nonlinear optimal control techniques for vibration attenuation using magnetostrictive actuators, *Journal of lntelligent Material Systems and Structures*, 19 (2) (2008) 193-209.

[18] M. A. Janaideh, S. Rakheja and C. Y. Su, A generalized Prandtl-Ishlinskii model for characterizing the hysteresis and saturation non linearities of smart actuators, *Smart Materials and Structures*, 18 (4) (2009) 1-9.

[19] J. Mao and H. Ding, Intelligent modeling and control for nonlinear systems with rate-dependent hysteresis, *Science in China*, 52 (4) (2009) 656-673.

[20] X. Chen, T. Hisayama and C. Y. Su, Pseudo-inverse-based adaptive control for uncertain discrete time systems preceded by hysteresis, *Automatica*, 45 (2) (2009) 469-476.

[21] P. Liu, Z. Zhang and J. Q. Mao, Modeling and control for giant magnetostrictive actuator with rate-dependent hysteresis, *Journal of Applied Mathematics* (2013) 1-8.

[22] O. Aljanaideh, S. Rakheja and C. Y. Su, Experimental characterization and modeling of rate-dependent asymmetric hysteresis of magnetostrictive actuators, *Smart Materials and Structures*, 23 (2014) 1-12.

[23] J. Liu, J. H. Liu and S. J. Dyke, Control-structure interaction for micro-vibration structural control, *Smart Materials and Structures*, Doi: https://doi.org/10.1088/0964-1726/21/10/105021.

Jinjun Jiang received the B.E., M.E. degrees in Mechanical Engineering and automatization from Hebei Engineering University in 2006 and 2009. From 2017 to 2018 he has been to New York University as a visiting scholar in Mechanical Engineering and Complex Network Control. Since 2009, he has been an engineer and researcher in China Aerospace Aerodynamics Academy. He is the author of more than 10 articles and holds more than 10 inventions patents. His research mainly focuses on mechatronics Control Technology, Complex Network, Industry Robot Control, Vibration Control Technology robotic structure and control, and human-machine system.

Weijin Gao received the Ph.D. in mechatronics engineering from Beihang University. Since 2016, he has been an engineer and researcher in China Aerospace Aerodynamics Academy. His research interests include dynamic topology optimization and active vibration control. He is the author of ten articles and holds three inventions patents.